Solubility and antisolvent crystallization of lithium hydroxide monohydrate in various organic solvents

Lien Lemmens,[a] Xavi Vanwezer,[a] Stijn Raiguel,[a] Rayco Lommelen,[a] Kerstin Forsberg,[b]

Tom Van Gerven,[c] Koen Binnemans*[a]

[a] KU Leuven, Department of Chemistry, Celestijnenlaan 200F, P.O. box 2404, B-3001 Leuven, Belgium

[b] KTH Royal Institute of Technology, Department of Chemical Engineering, Stockholm, Sweden

[c] KU Leuven, Department of Chemical Engineering, Celestijnenlaan 200F, P.O. Box 2424, B-3001 Leuven, Belgium

Supplementary Information (SI)

*Corresponding author:

Email address: Koen.Binnemans@kuleuven.be

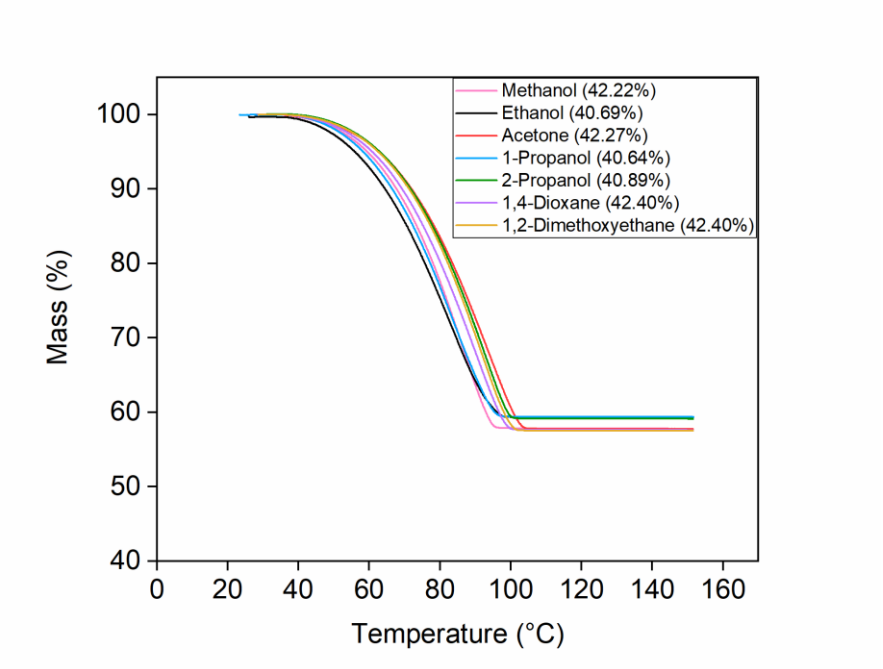

Fig. S1. TGA curves showing the percentage mass loss as a function of temperature for the solid phases obtained from solubility experiments using different antisolvents at an O/A ratio of 1/10.

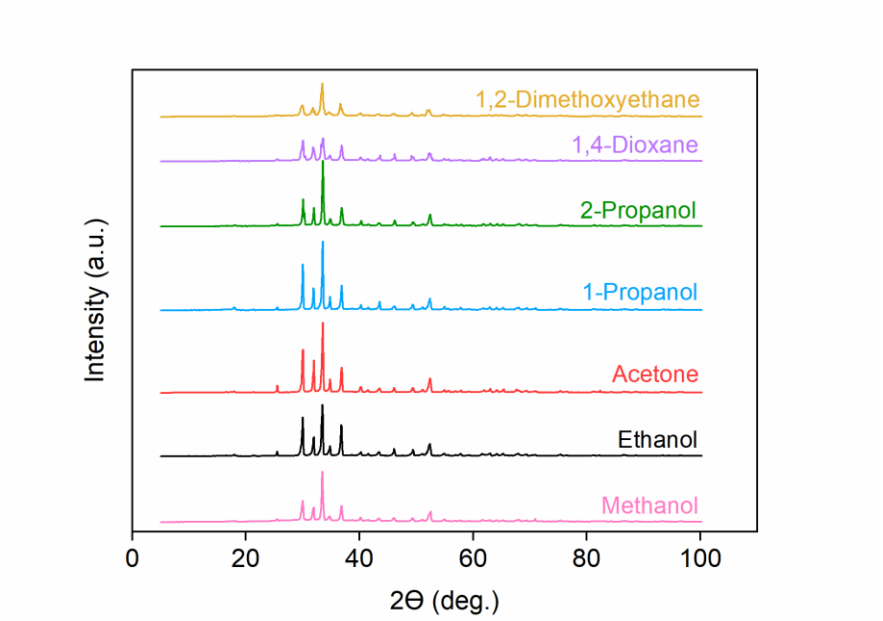

Fig. S2. XRD diffractograms confirming the presence of $LiOH \cdot H_2O$ using different antisolvents at an O/A ratio of 1/10.

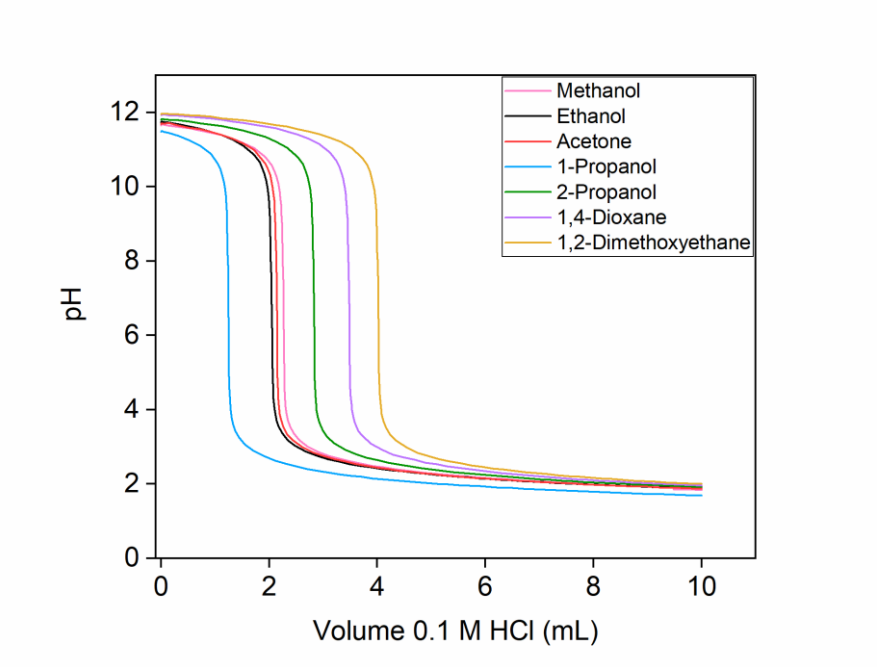

Fig. S3. Titration curves with single equivalence points, indicating no significant formation of Li_2CO_3 using different antisolvents at an 1/10 O/A ratio.

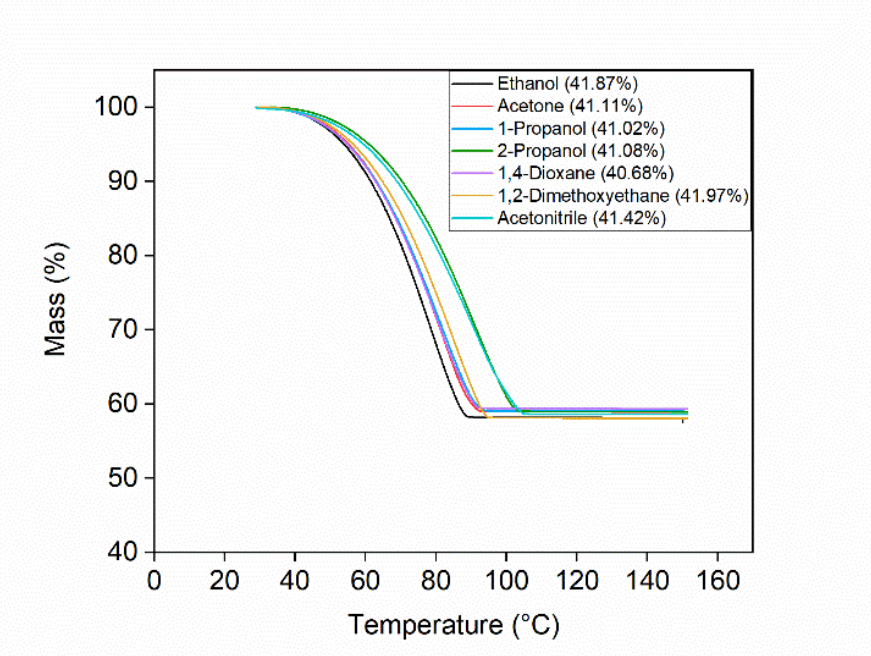

Fig. S4. TGA curves showing the percentage mass loss as a function of temperature for the solid phases obtained from solubility experiments using different antisolvents at an O/A ratio of 6/1.

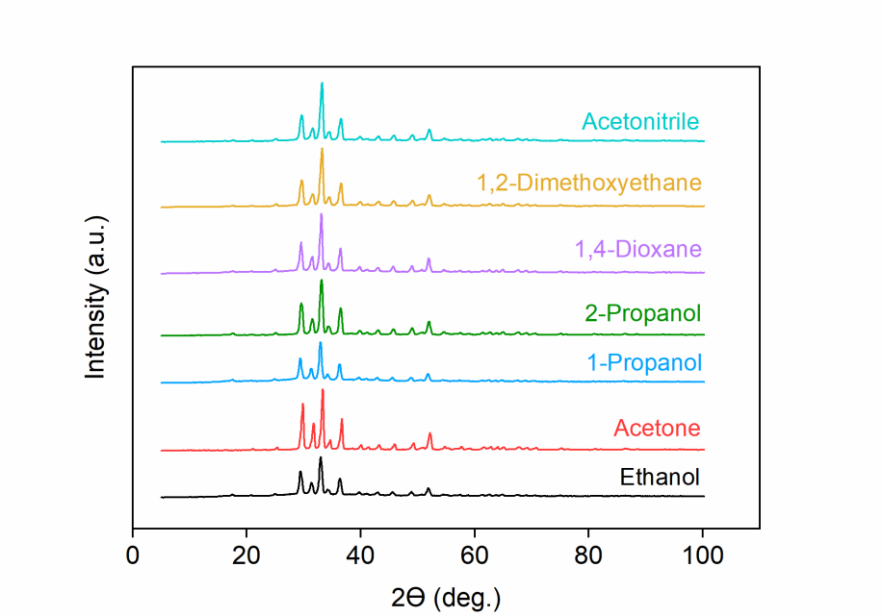

Fig. S5. XRD diffractograms confirming the presence of $LiOH \cdot H_2O$ using different antisolvents at an O/A ratio of 6/1.

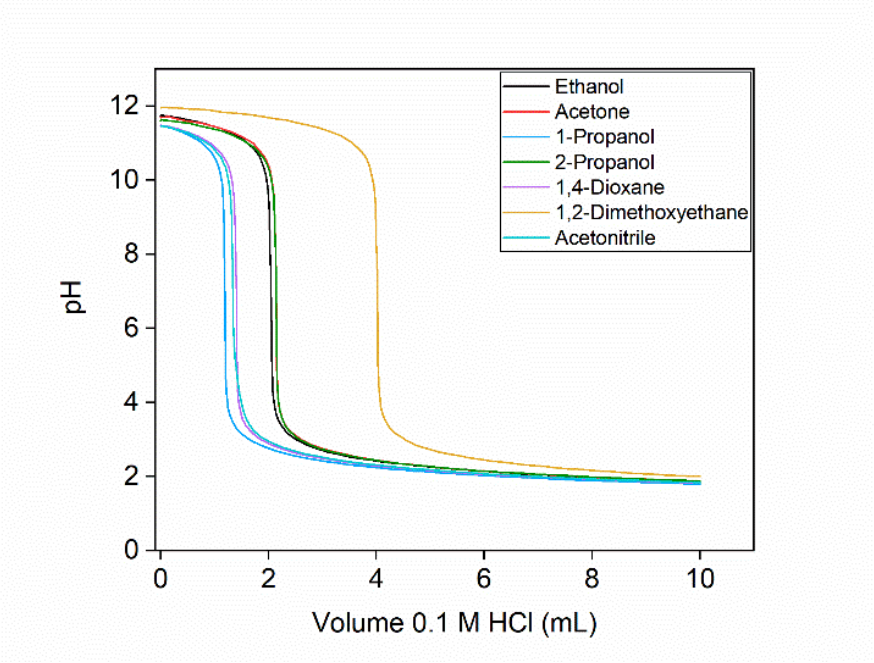

Fig. S6. Titration curves with single equivalence points, indicating no significant formation of Li_2CO_3 using different antisolvents at an 6/1 O/A ratio.

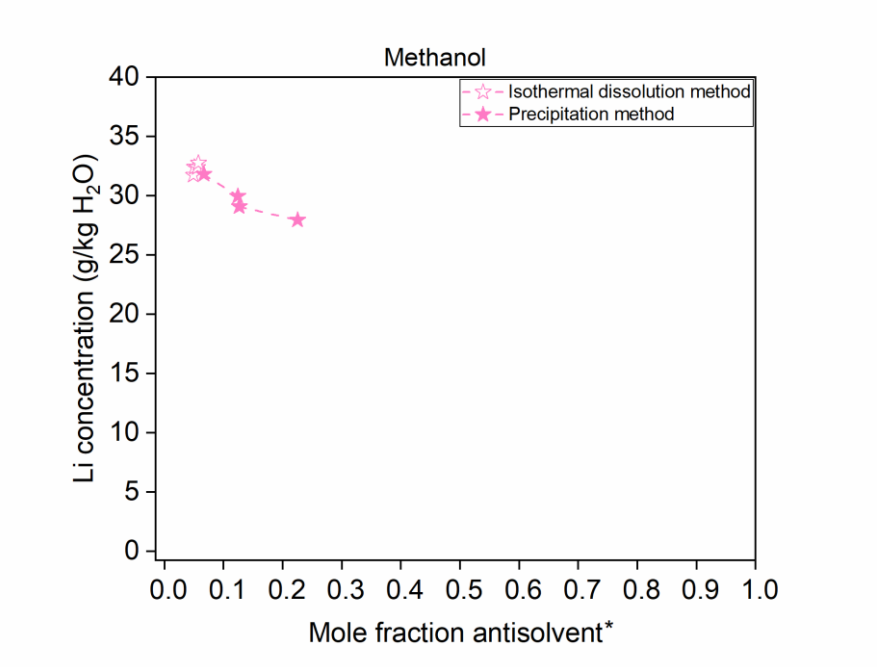

Fig. S7. Lithium concentration in LiOH–water–methanol mixtures at 25 °C as a function of the mole fraction of methanol. *Mole fraction of antisolvent at equilibrium.

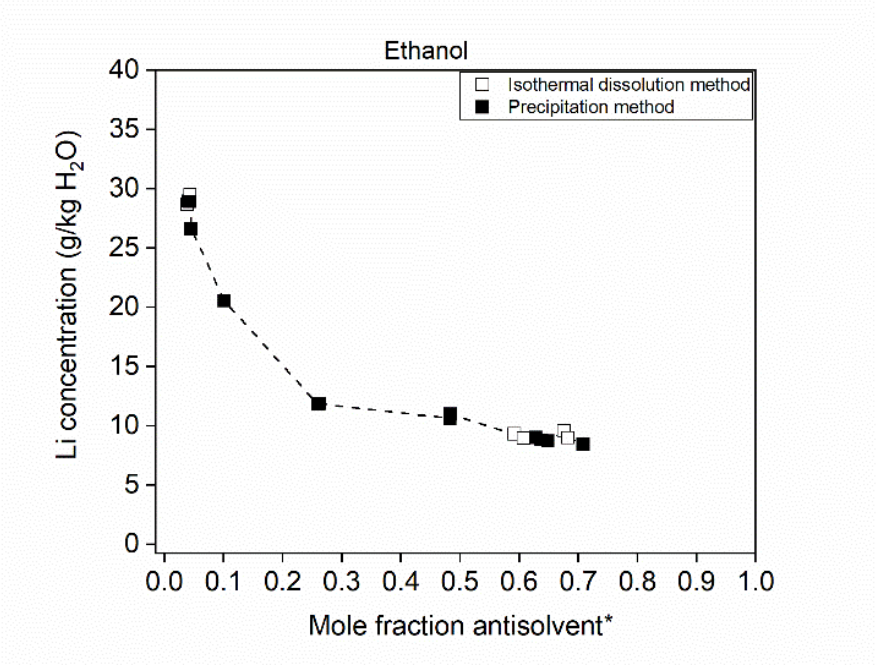

Fig. S8. Lithium concentration in LiOH–water–ethanol mixtures at 25 °C as a function of the mole fraction of ethanol. *Mole fraction of antisolvent at equilibrium.

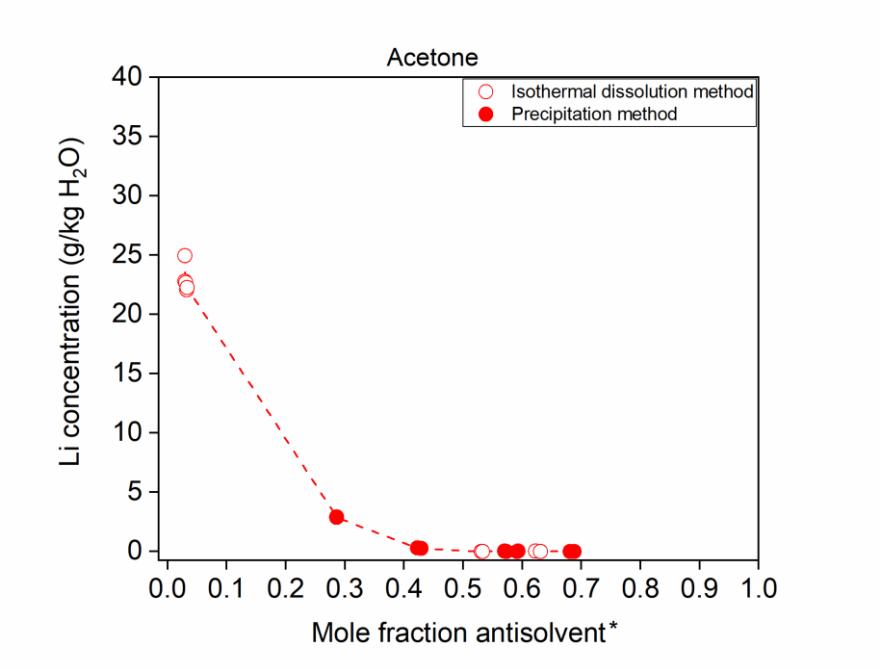

Fig. S9. Lithium concentration in LiOH–water–acetone mixtures at 25 °C as a function of the mole fraction of acetone. *Mole fraction of antisolvent at equilibrium.

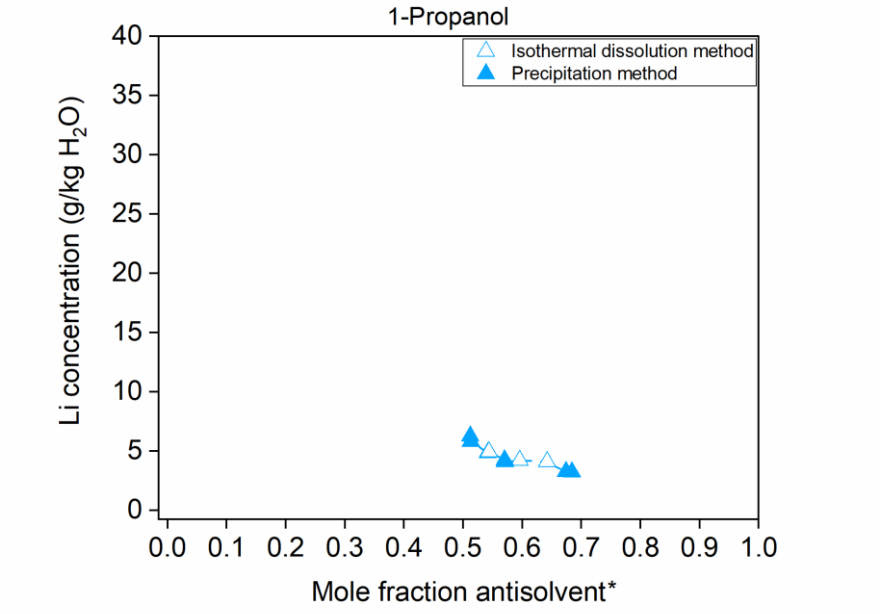

Fig. S10. Lithium concentration in LiOH–water–1-propanol mixtures at 25 °C as a function of the mole fraction of 1-propanol. *Mole fraction of antisolvent at equilibrium.

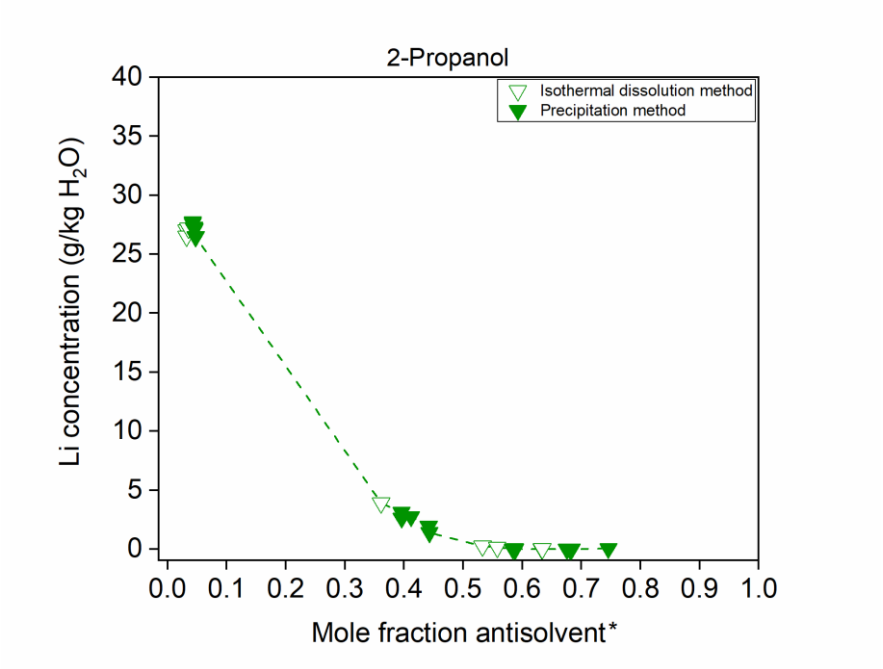

Fig. S11. Lithium concentration in LiOH–water–2-propanol mixtures at 25 °C as a function of the mole fraction of 2-propanol. *Mole fraction of antisolvent at equilibrium.

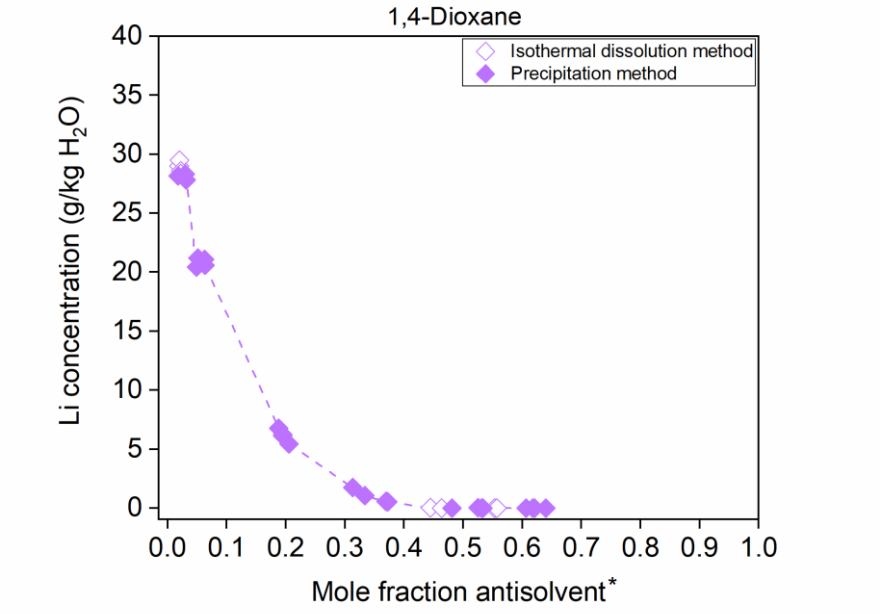

Fig. S12. Lithium concentration in LiOH–water–dioxane mixtures at 25 °C as a function of the mole fraction of dioxane. *Mole fraction of antisolvent at equilibrium.

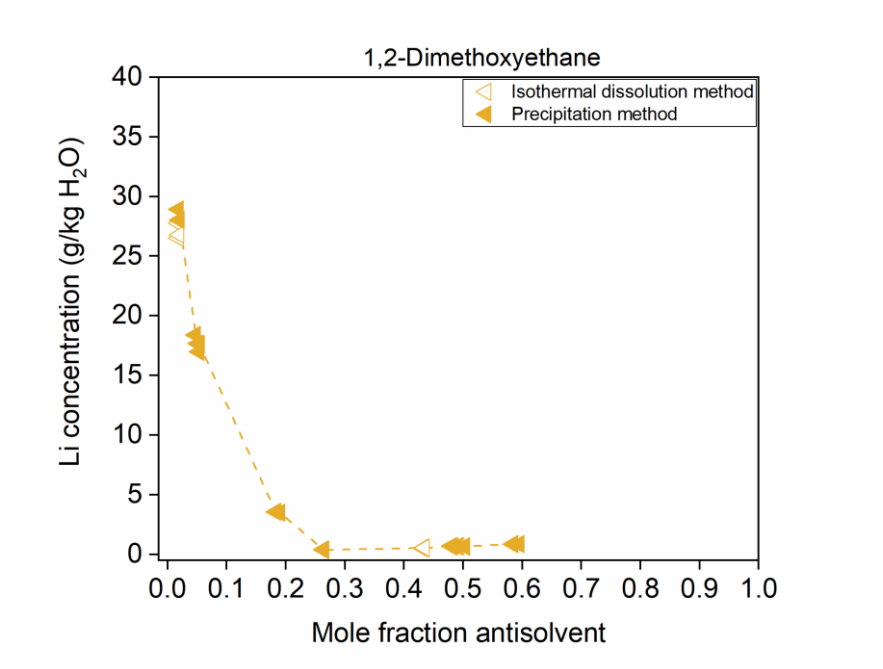

Fig. S13. Lithium concentration in LiOH–water–DME mixtures at 25 °C as a function of the mole fraction of DME. *Mole fraction of antisolvent at equilibrium.

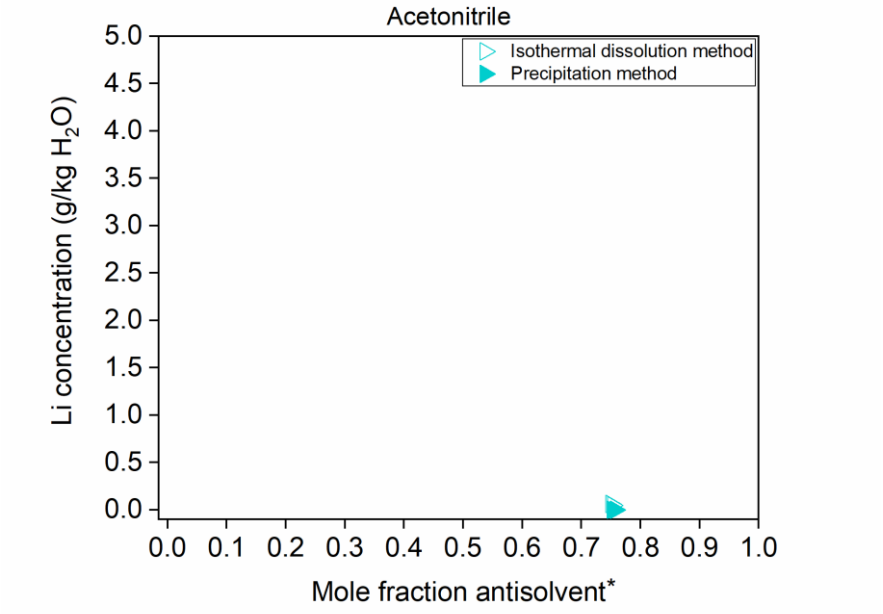

Fig. S14. Lithium concentration in LiOH–water–acetonitrile mixtures at 25 °C as a function of the mole fraction of acetonitrile. *Mole fraction of antisolvent at equilibrium.

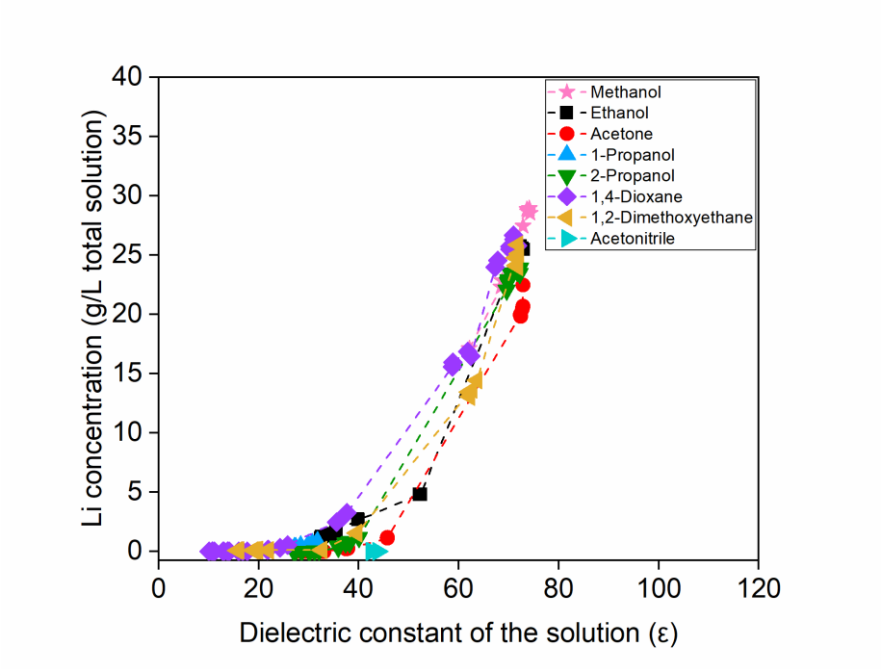

Fig. S15. Lithium concentration as a function of the dielectric constant of the solvent mixture.

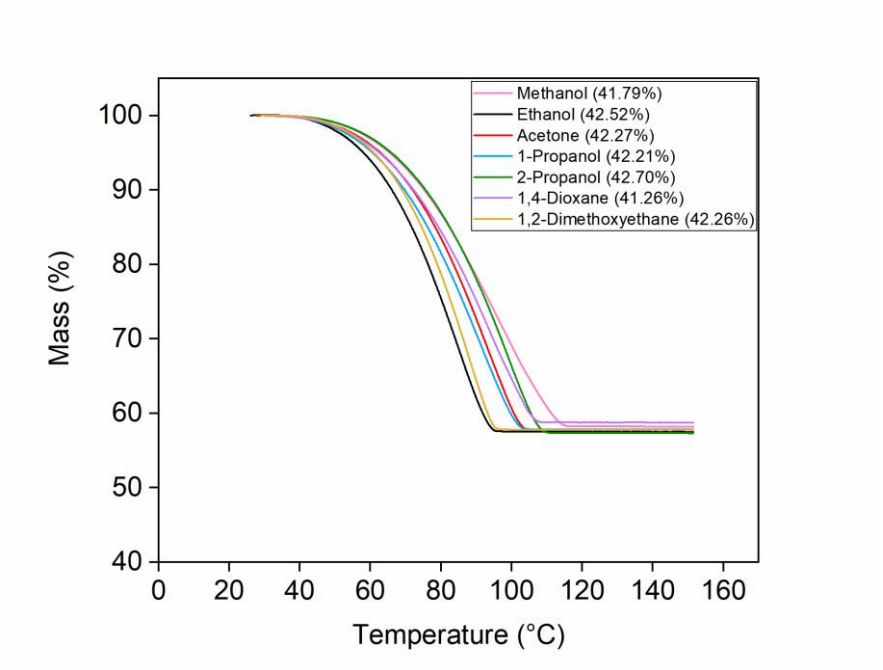

Fig. S16. TGA curves showing the percentage mass loss as a function of temperature for the solid phases obtained from solubility experiments using different antisolvents at an O/A ratio of 1/4.

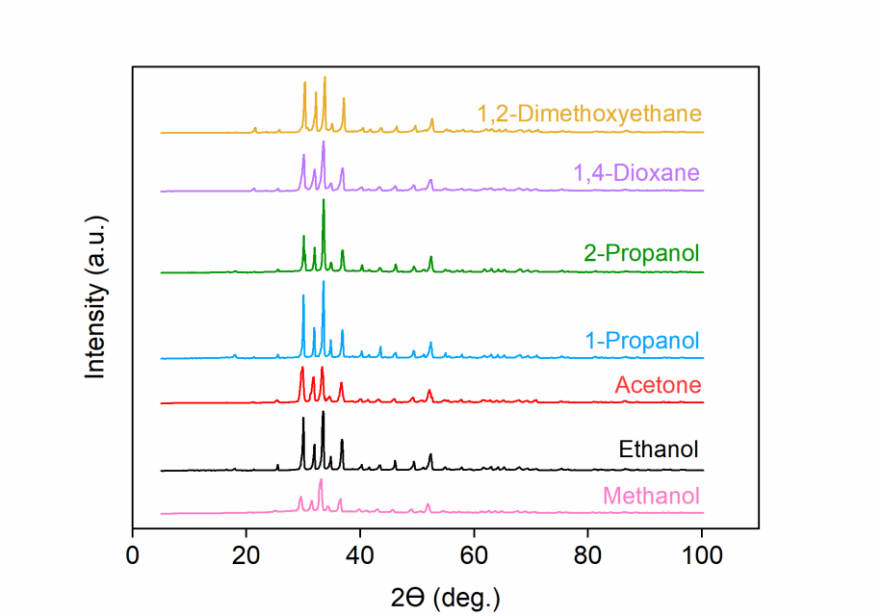

Fig. S17. XRD diffractograms confirming the presence of $LiOH \cdot H_2O$ using different antisolvents at an O/A ratio of 1/4.

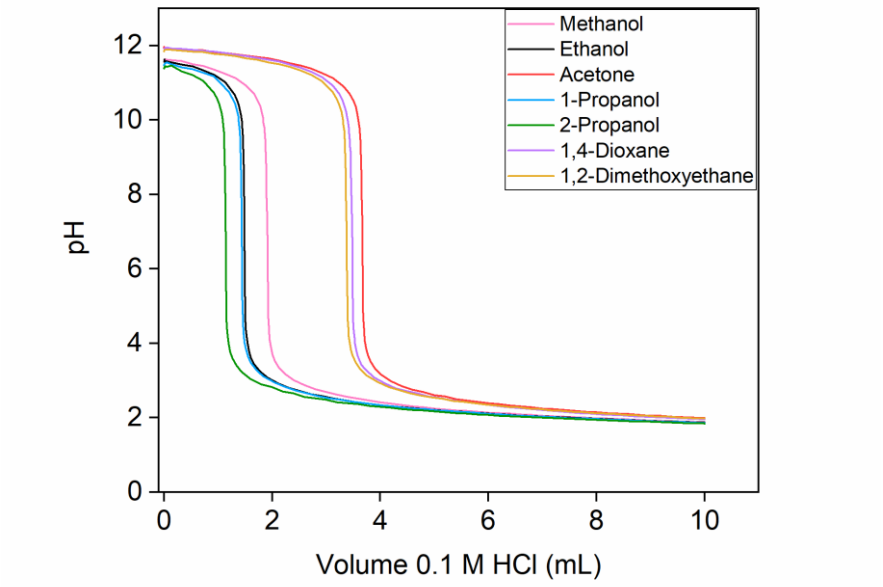

Fig. S18. Titration curves with single equivalence points, indicating no significant formation of Li_2CO_3 using different antisolvents at an 1/4 O/A ratio.

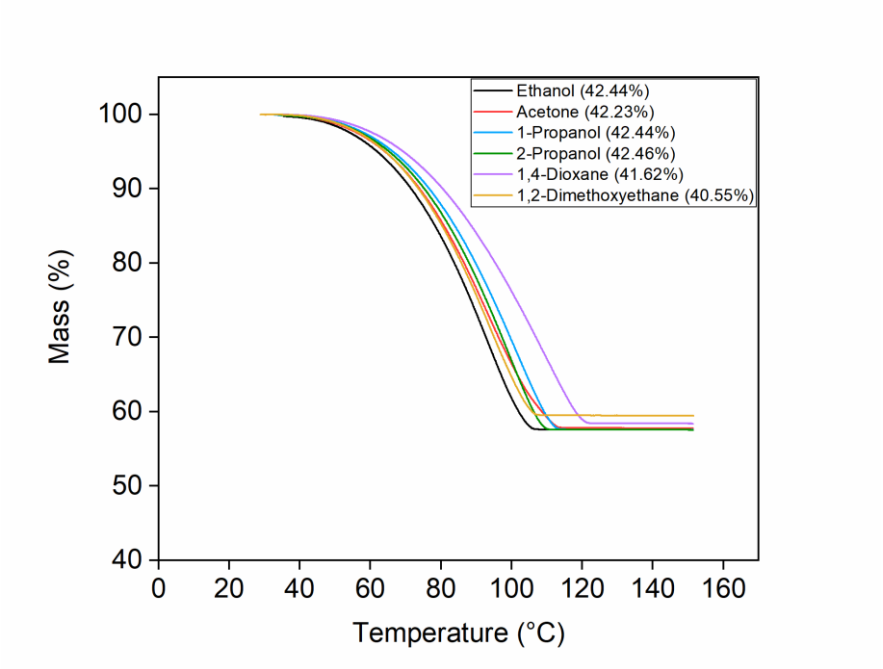

Fig. S19. TGA curves showing the percentage mass loss as a function of temperature for the solid phases obtained from solubility experiments using different antisolvents at an O/A ratio of 1/1.

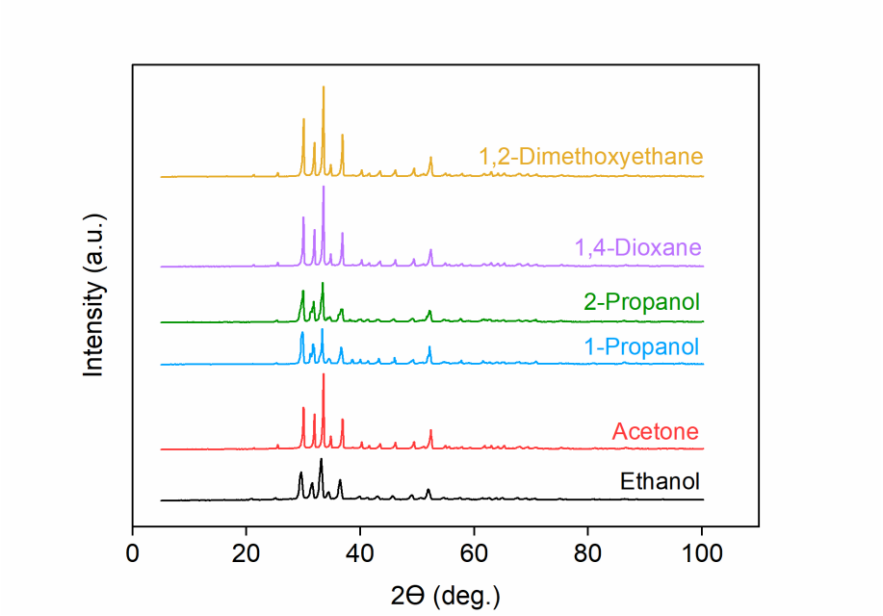

Fig. S20. XRD diffractograms confirming the presence of $LiOH \cdot H_2O$ using different antisolvents at an O/A ratio of 1/1.

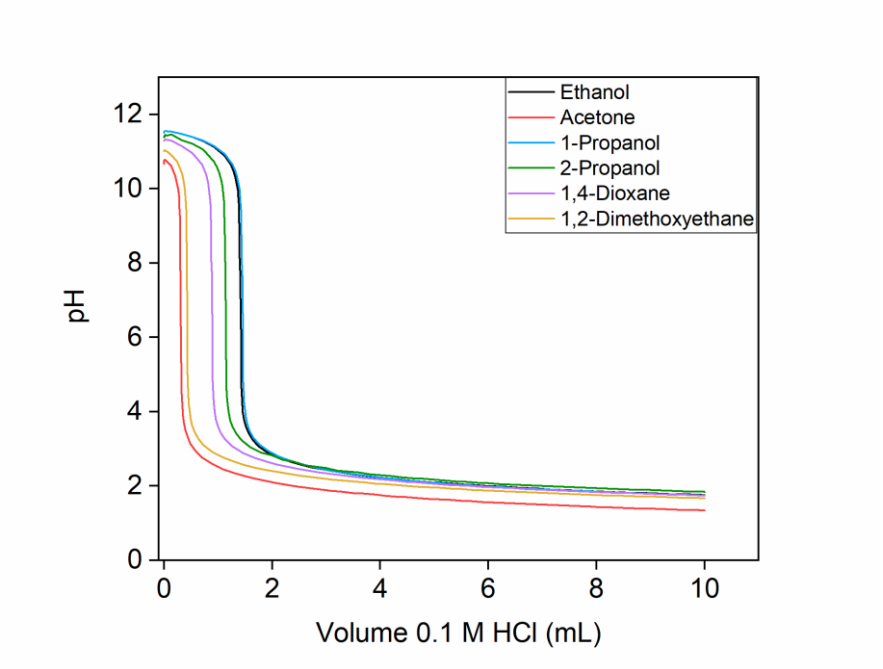

Fig. S21. Titration curves with single equivalence points, indicating no significant formation of Li_2CO_3 using different antisolvents at an 1/1 O/A ratio.

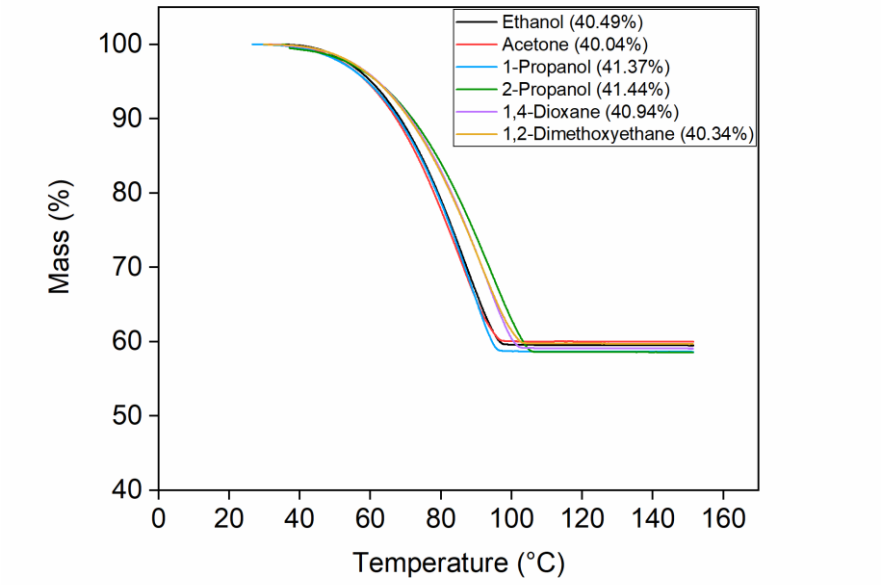

Fig. S22. TGA curves showing the percentage mass loss as a function of temperature for the solid phases obtained from solubility experiments using different antisolvents at an O/A ratio of 4/1.

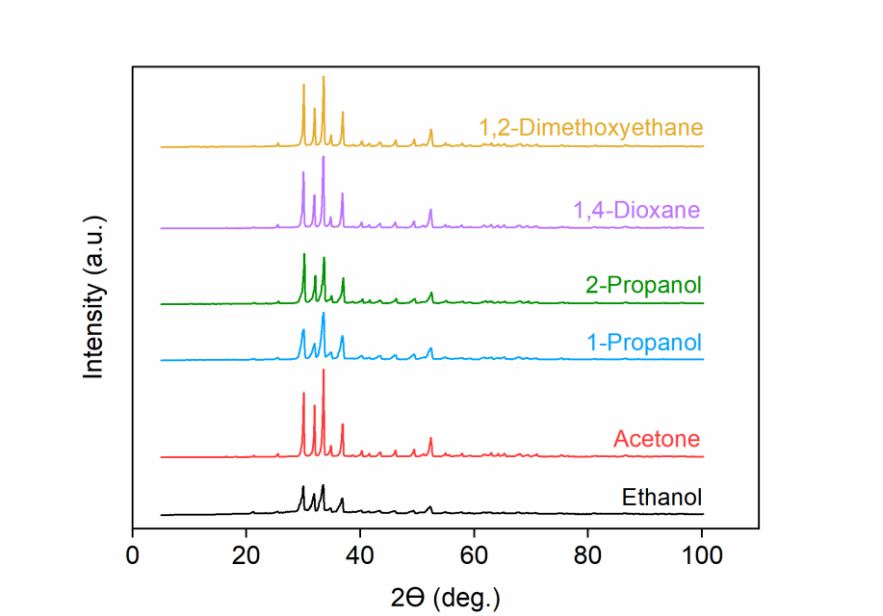

Fig. S23. XRD diffractograms confirming the presence of $LiOH \cdot H_2O$ using different antisolvents at an O/A ratio of 4/1.

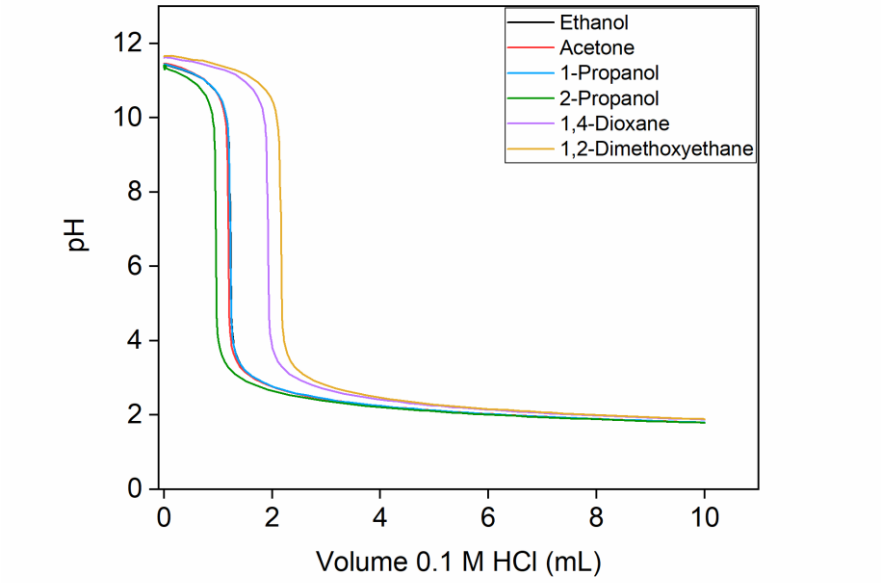

Fig. S24. Titration curves with single equivalence points, indicating no significant formation of Li_2CO_3 using different antisolvents at an 4/1 O/A ratio.

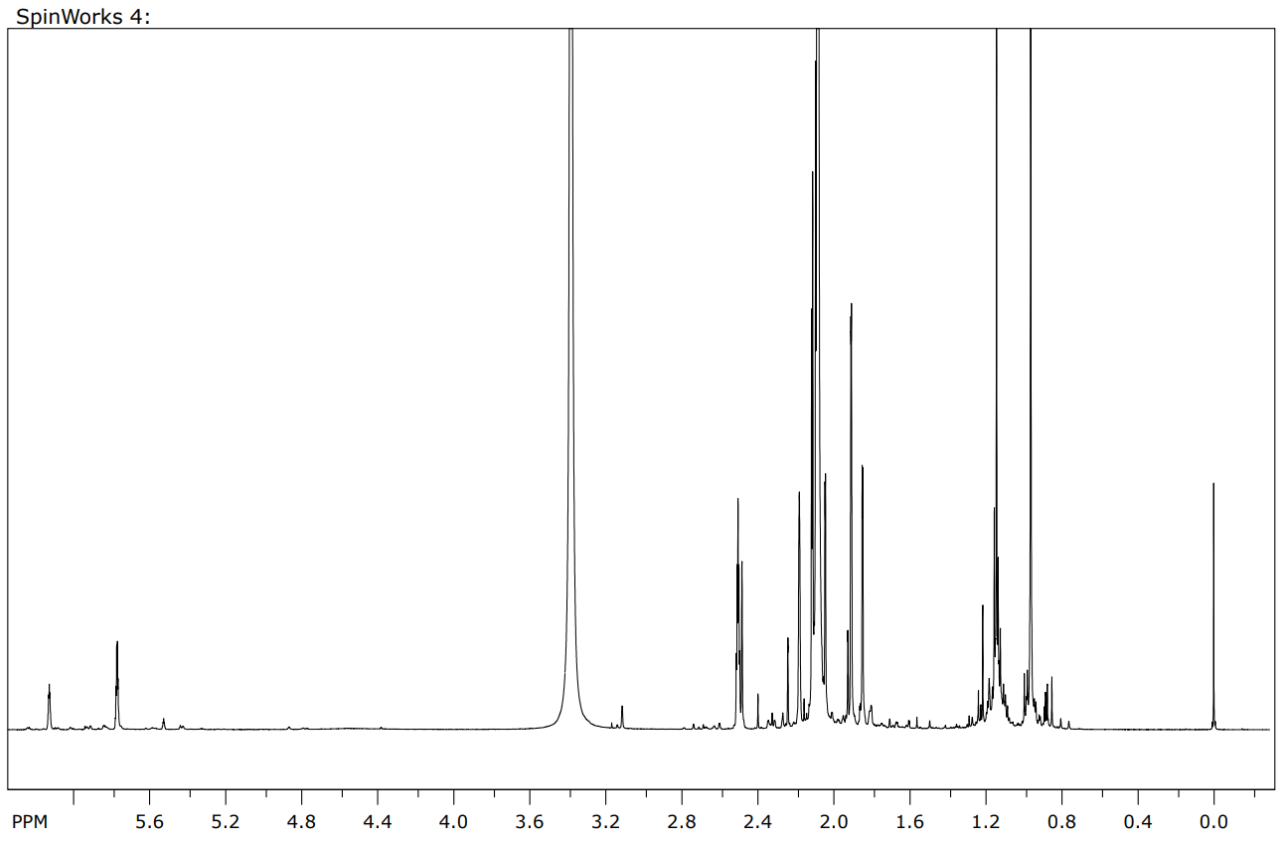

Fig. S25. ^{1}H NMR spectrum of the product mixture obtained from acetone in an alkaline environment, showing numerous additional peaks alongside water (≈ 3.38 ppm) and acetone (≈ 2.09 ppm), consistent with products of aldol condensation. Spectrum recorded on a Bruker Avance III + operating at 400 MHz in $(CD_3)_2SO$.

Table S1. Phase composition, density, and water content of the lower and upper phases in the two liquid phase system of acetonitrile.[1]

	Acetonitrile				
	LiOH mole fraction	H_2O mole fraction	Antisolvent mole fraction	Density (kg/L)	Water content (%) by KF
Lower phase	6.32	93.68	< DL*	1.07	74.36
Upper phase	0.024	25.07	74.91	0.80	12.80

[1]Mole fractions are normalized such that the sum of LiOH, H_2O, and antisolvent equals 100%. According to the Gibbs phase rule, at constant temperature and pressure the system has no degrees of freedom. Therefore, the compositions of the lower and upper phases are fixed and independent of the O/A mass ratios investigated.
*DL indicates concentrations below the detection limit of the GC-MS method.

Table S2. Data for the ternary phase diagrams of the LiOH – water – antisolvent systems at 25 °C under equilibrium conditions. All compositions are normalized such that the sum of the three components equals 100%, while the ternary diagrams in the main text are displayed on a mole fraction scale ranging from 0 to 1.

Methanol			**Ethanol**			**Acetone**			**1-Propanol**		
LiOH mole fraction	H_2O mole fraction	Antisolvent mole fraction	LiOH mole fraction	H_2O mole fraction	Antisolvent mole fraction	LiOH mole fraction	H_2O mole fraction	Antisolvent mole fraction	LiOH mole fraction	H_2O mole fraction	Antisolvent mole fraction
7.24	87.88	4.88	6.65	89.48	3.87	5.90	91.12	2.98	1.19	47.61	51.20
7.36	87.56	5.08	6.70	89.22	4.08	5.41	91.61	2.98	1.19	47.61	51.20
7.32	87.12	5.56	6.79	88.84	4.37	5.38	91.53	3.09	0.47	42.50	57.02
7.39	86.90	5.71	2.20	71.80	26.00	5.24	91.50	3.26	0.45	42.49	57.06
7.12	86.22	6.67	2.20	71.57	26.22	5.28	91.40	3.32	0.44	39.99	59.57
6.32	81.30	12.37	1.39	50.27	48.34	0.54	70.86	28.61	0.38	35.45	64.17
6.19	81.17	12.65	1.43	50.13	48.44	0.53	70.85	28.62	0.27	32.33	67.39
5.24	72.25	22.51	0.96	39.79	59.25	0.041	57.64	42.32	0.26	31.33	68.40
			0.89	38.34	60.77	0.038	57.06	42.90			
			0.85	36.32	62.83	0.00060	46.90	53.10			
			0.81	35.40	63.79	0.00050	46.71	53.29			
			0.79	31.60	67.61	0.0037	42.94	57.06			
			0.72	31.04	68.24	0.00044	42.68	57.32			
						0.00044	40.85	59.15			
						0.0034	40.68	59.31			
						0.0010	37.70	62.30			
						0.00035	36.90	63.10			
						0.00014	31.91	68.09			
						0.00019	31.20	68.80			

2-Propanol			**1,4-Dioxane**			**1,2-Dimethoxyethane**			**Acetonitrile**		
LiOH mole fraction	H_2O mole fraction	Antisolvent mole fraction	LiOH mole fraction	H_2O mole fraction	Antisolvent mole fraction	LiOH mole fraction	H_2O mole fraction	Antisolvent mole fraction	LiOH mole fraction	H_2O mole fraction	Antisolvent mole fraction
6.35	90.46	3.19	6.69	91.53	1.78	6.60	91.60	1.80	0.0040	24.98	75.01
6.23	90.56	3.21	6.86	91.16	1.98	6.85	91.30	1.85	0.0000051	24.73	75.27
6.36	90.13	3.51	6.97	91.02	2.01	6.32	91.82	1.86	0.0029	24.66	75.33
6.41	89.36	4.24	6.75	91.02	2.23	6.37	91.68	1.95	0.0000076	24.21	75.79
6.42	89.33	4.24	6.70	91.07	2.23	6.65	91.36	2.00			
6.31	89.19	4.50	6.64	90.39	2.98	4.34	90.92	4.74			
6.29	89.20	4.51	6.52	90.33	3.15	4.00	90.69	5.31			
6.27	89.14	4.59	4.79	90.32	4.89	4.13	90.47	5.40			
6.12	89.13	4.74	4.94	89.92	5.13	0.74	80.05	19.21			
0.48	59.96	39.56	4.86	88.87	6.27	0.73	80.20	19.07			
0.41	59.96	39.63	4.75	88.92	6.32	0.074	73.57	26.35			
0.42	58.39	41.20	1.40	79.81	18.79	0.070	73.45	26.48			
0.28	55.54	44.18	1.29	79.23	19.49	0.079	56.75	43.18			
0.20	55.51	44.29	1.26	79.23	19.51	0.079	56.46	43.46			
0.031	46.69	53.28	1.11	78.34	20.55	0.093	51.94	47.97			
0.014	44.24	55.74	0.31	68.39	31.30	0.092	51.58	48.33			
0.0000089	41.58	58.42	0.18	66.47	33.35	0.089	50.83	49.08			

0.00069	41.26	58.74	0.090	63.00	36.91	0.089	50.67	49.24
0.00045	41.21	58.79	0.085	62.69	37.23	0.090	50.62	49.29
0.00073	36.71	63.29	0.0028	55.57	44.43	0.090	49.64	50.27
0.0017	36.60	63.40	0.0022	53.61	46.39	0.083	49.61	50.31
0.000051	32.44	67.56	0.0013	46.85	53.14	0.093	41.51	58.39
0.000074	31.90	68.10	0.0020	51.88	48.12	0.091	40.41	59.50
0.0000050	31.66	68.34	0.0019	46.64	53.36			
			0.0019	44.70	55.30			
			0.00085	44.31	55.69			
			0.00042	39.35	60.65			
			0.00033	38.23	61.77			
			0.00086	37.94	62.06			
			0.00051	36.02	63.98			